

See discussions, stats, and author profiles for this publication at: <https://www.researchgate.net/publication/326098616>

Performance-based Seismic Risk Assessment of Urban Systems

Article in *International Journal of Architectural Heritage* · July 2018

DOI: 10.1080/15583058.2018.1503371

CITATIONS

16

READS

322

4 authors, including:



Alberto Basaglia

Università degli Studi G. d'Annunzio Chieti e Pescara

5 PUBLICATIONS 19 CITATIONS

[SEE PROFILE](#)



Alessandra Aprile

University of Ferrara

48 PUBLICATIONS 761 CITATIONS

[SEE PROFILE](#)



Francesco Pilla

University College Dublin

113 PUBLICATIONS 852 CITATIONS

[SEE PROFILE](#)

Some of the authors of this publication are also working on these related projects:



Stability of Structures under their Own Weight [View project](#)



Forest fire impact on ecosystem & Environment [View project](#)

1 **PERFORMANCE-BASED SEISMIC RISK ASSESSMENT OF**
2 **URBAN SYSTEMS**
3 **(Running Head)**
4

5 **Alberto Basaglia¹, Alessandra Aprile², Enrico Spacone¹ and Francesco Pilla³**

6 ¹Department of Engineering and Geology, University of Chieti - Pescara

7 Viale Pindaro 42, 65127 Pescara, Italy

8 e-mail: {alberto.basaglia@unich.it ; esacone@unich.it}

9 ²Department of Engineering, University of Ferrara

10 Via Saragat 1, 44122 Ferrara, Italy

11 e-mail: alessandra.aprile@unife.it

12 ³Department of Planning and Environmental Policy, University College Dublin

13 Richview, Clonskeagh, Dublin, Ireland

14 e-mail: francesco.pilla@ucd.ie
15

16
17
18
19
20
21
22
23
24
25
26
27
28
29
30
31
32
33
34
35
36
37
38
39
40

ABSTRACT

Disaster risk mitigation has become a global urgent need. Similarly to other natural hazards, earthquakes may cause significant damage on a large scale. In Europe and in other regions with dense urbanization, seismic events can heavily impact historical city centres due to the several structural fragilities. These centers are often part of the worldwide cultural heritage and their preservation is considered a strategic issue. Furthermore, earthquakes may have severe negative short-term economic effects on the impacted communities and adverse longer-term consequences for economic growth. For this reason, the development of an efficient approach for urban seismic risk assessment becomes essential. An original approach is proposed, based on performance concepts and multidisciplinary perspectives. The procedure is applied for validation to the city center of Concordia Sulla Secchia (Italy), damaged by the 2012 Pianura Padana Earthquake (PPE), comparing predicted damage scenarios with the actual post-seismic survey data.

KEYWORDS: seismic risk, risk assessment, risk mitigation, performance-based assessment, cultural heritage protection, GIS applications

41 1. INTRODUCTION

42 With the approval of the “Sendai Framework 2015-2030 (UNISDR 2015)” the U.N. has
43 declared disaster risk reduction one of the biggest global challenges the world deals with today,
44 and has proposed unified guidelines for risk reduction and disaster management. In recent years,
45 natural disasters have affected the world population in repeated and severe ways. Among all
46 catastrophic events, strong earthquakes typically produce damage on a vast scale in areas of
47 high hazard and poor construction techniques. They may cause a high number of casualties,
48 severe economic losses and are a major threat to cultural heritage sites.

49 In Europe, historical city centres represent an essential part of the cultural heritage. Their
50 dense urban structure, made of ancient masonry buildings, often built in aggregate, and pre-
51 modern seismic code Reinforced Concrete (RC) constructions, make them highly vulnerable.
52 This immeasurable cultural heritage is considered by the EU a “strategic resource for a
53 sustainable Europe” that needs to be preserved (CotEU 2014). Among all European countries,
54 Italy has the highest number of UNESCO listed heritage sites (source: UNESCO website). From
55 1968 to date, the Italian central government has spent more than 120 billion Euros for
56 reconstruction costs in the aftermath of major seismic events (Di Mauro 2014), with a
57 significant impact on the Nation’s economic budget. The development of practical seismic risk
58 assessment tools could lead up to the preventive planning of retrofit works, aimed at minimizing
59 casualties and damage.

60 In literature, many definitions of the seismic risk for a single element of the city (for
61 example a building) can be found. One of the most complete definition is related to the PEER
62 methodology (Porter 2003), leading to:

$$\lambda(DV) = \iiint G\langle DV|DM \rangle dG\langle DM|EDP \rangle dG\langle EDP|IM \rangle d\lambda(IM) \quad (1)$$

63 Where, from right to left, four different terms can be distinguished:

64 $d\lambda(IM)$ refers to the **hazard** characterization of the area under assessment, determining
65 the probability of occurrence of seismic events and their expected Intensity Measure, IM.
66 Among all possible intensity measures, the mainly used are: the peak ground acceleration, pga
67 [unit measure: g], the spectral acceleration, S_a [g's], and the European Macroseismic
68 Intensities, I_{EMS-98} [-] (Grünthal et. al. 1998);

69 $dG\langle EDP|IM \rangle$ refers to the **vulnerability** measure of the building under assessment given
70 the hazard defined above (i.e. conditional probability). The vulnerability is the intrinsic
71 predisposition to suffer structural damage after a seismic event, and the damage can be
72 expressed using different Engineering-Demand Parameter, EDP (for example interstorey drift);

73 $dG\langle DM|EDP \rangle$ refers to the **damage** definition of the building under assessment given the
74 vulnerability measure defined above (i.e. conditional probability). Damage parameter, DM, can
75 be expressed using appropriate models , such as, for example, the interstorey drift ratios
76 proposed by Ghobarah (2004) or the total displacement thresholds introduced by Lagomarsino
77 and Giovinazzi (2006);

78 $G\langle DV|DM \rangle$ refers to the **loss** evaluation given the damage defined above (i.e. conditional
79 probability). Losses are herein described as a Decision Variable, DV, because, depending on
80 their entity, the evaluated risk level can be defined as *acceptable* or not.

81 The hazard characterization is usually performed using maps provided by Public
82 Authorities. For example, the Italian National Institute of Geophysics and Volcanology (INGV)
83 produces and updates an interactive hazard map of the Italian territory. More detailed
84 assessment may include also specific data on site effects, like spectral amplification or
85 liquefaction probability (Bramerini et al. 1995; McGuire 2004).

86 The vulnerability measure of buildings can be performed following different methods. The
87 most accurate approach is based on structural response evaluation through Finite Element
88 Modelling (FEM) analyses. This approach is referred to as **direct method**. It requires a highly

89 detailed knowledge of the construction technique and may be time-consuming, depending on
90 the FEM model complexity. Examples of this approach are the work of Lang and Bachmann
91 (2003) and D’Ayala and Kishali (2012) that used non-linear analysis methods to study the in-
92 plane and out-of-plane behaviour of unreinforced masonry (URM) buildings. A less accurate
93 but more practical approach is represented by the so-called **indirect methods**. Their main
94 advantage is they grant a swift evaluation and can be used when details regarding the
95 construction technique are missing, for example when dealing with historical buildings. These
96 methods attribute the vulnerability level by dividing constructions in *classes*, or by using
97 *typological indicators*. An example of classes attribution is the classification proposed within
98 the EMS-98 approach (Grünthal et al. 1998). Buildings are divided into 6 *Vulnerability Classes*,
99 from A to F, where the most vulnerable constructions belong to Class A.

100 An example of typological indicators application is given by the *Vulnerability Index*
101 *Method*, originally introduced by Benedetti and Petrini (1984) and then developed, among the
102 others, by GNDT (GNDT-SSN 1994; CETE Méditerranée 2008) and Ferreira, Romeu and
103 Varum (2014) for masonry buildings and Podestà and Romano (2014) for RC structures. This
104 method uses standard forms, based on in-situ post-earthquake damage surveys, to evaluate the
105 buildings’ vulnerability level by considering 11 parameters (see Table I and Table II). Each
106 parameter represents one of the main features that influence the buildings’ response to a seismic
107 event. Parameters are ranged into classes of increasing vulnerability level by means of assigned
108 score, C_{vi} , and have an assigned weight, w_i . The weight denotes the different impact of
109 parameters on the overall seismic vulnerability - a higher weight meaning a higher influence.
110 Vulnerability classes of masonry buildings parameters are A-B-C-D. Vulnerability classes of
111 RC buildings parameters are A-B-C, with the exception of the 11-th parameter with the
112 additional class D. To assign a class and the related score to every parameter, buildings’
113 inspection are required, considering both geometrical and structural aspects. Once all classes

114 and scores are determined, the vulnerability index, I_V , is computed as a weighted sum of all the
115 parameters' scores, normalized in the range [0 – 100].

116 The choice between direct and indirect methods depends primarily on the number of
117 buildings under assessment, see Fig. 1. In fact, direct methods have a high accuracy, but they
118 can be extremely time-consuming. Therefore, when dealing with a large number of buildings
119 (from the building's aggregate to the whole city), the use of indirect methods becomes essential
120 even if it implies to accept a certain level of uncertainty of the results.

121 The damage definition is usually performed applying a probabilistic approach. For
122 example, outputs of direct and indirect methods are used to derive *fragility curves* (Porter 2017).
123 Fragility curves are cumulative distribution functions that express the probability of a building
124 to exceed defined damage levels for increasing value of the PGA. First the American *Applied*
125 *Technology Council* (ATC), introduced a fragility curve database (Anagnos, Rojahn and
126 Kiremidjian 1995). Similarly, the European research projects RISK-UE (Mouroux et al. 2004;
127 Lantada et al. 2010) and SYNER-G (2011) proposed a framework to produce earthquake
128 scenarios and perform loss assessments. Then, the *Federal Emergency Management*, or FEMA,
129 developed and has been constantly updating HAZUS (FEMA 2015), a tool to assess the seismic
130 losses for both the built environment and population using *capacity curves* (Chopra and Goel
131 1999; Bertero 2000). A capacity curve, is the plot of a building's lateral load resistance as a
132 function of a lateral displacement (i.e., a force-deflection plot), and values are usually expressed
133 in terms of spectral acceleration, S_a , and spectral displacement, S_d .

134 Another approach to damage is given by the so-called *Macroseismic Method* (Giovinazzi
135 and Lagomarsino 2004; Giovinazzi 2005; Lagomarsino and Giovinazzi, 2006), that derives by
136 the introduction of the EMS-98 scale (Grünthal et. al. 1998). In fact, following the EMS-98
137 approach, a qualitative description of the expected damage level, $D_k = [0, 5]$ (0 = no damage,
138 5 = collapse) is used, for each vulnerability class and for increasing seismic intensities, I_{EMS-98} .

139 Within the macroseismic method, the expected damage level descriptions are used to define
 140 Damage Probability Matrixes (DPMs) that return the expected probability of undergoing a
 141 damage level for given vulnerability class and seismic intensity. Then, DPMs results are
 142 described using a single parameter: the Vulnerability, V . In this way, it is possible to associate
 143 a numerical value to each Vulnerability class, as reported in Bernardini et al. (2007).
 144 Vulnerability, V , is used to evaluate the mean damage grade, $\mu_D = [0, 5]$ (0 = no damage, 5 =
 145 collapse) using the following Eqs. 2 and 3 (Lagomarsino and Giovinazzi 2006):

$$\mu_D = 2.5 \cdot \left[1 + \tanh \left(\frac{I_{EMS-98} + 6.25 \cdot V - 13.1}{Q} \right) \right] \cdot f(I_{EMS-98}, V) \quad (2)$$

$$f(I_{EMS-98}, V) = \begin{cases} e^{\frac{V}{2} \cdot (I_{EMS-98} - 7)} & I_{EMS-98} \leq 7 \\ 1 & I_{EMS-98} > 7 \end{cases} \quad (3)$$

146 Where:

- 147 ▪ Q is a ductility factor, defined equal to 2.3 for masonry buildings and in the $[2.3 \div 3.3]$ range
 148 for RC buildings depending the seismic code level and the regularity in height (Lagomarsino
 149 and Giovinazzi 2006)
- 150 ▪ $f(I_{EMS-98}, V)$ is a corrective function to better describe the damage for lower intensities
 151 (Bernardini et al. 2007).

152 The buildings' damage distribution is subsequently defined through a probabilistic
 153 approach. In particular, Giovinazzi (2005) introduce the beta probability distribution function,
 154 $p_\beta(x)$, whose Probability Density Function (PDF) and Cumulative Density Function (CDF) are
 155 reported by Eqs. 4 and 5. The damage level x is assumed as a continuous variable and μ_x and
 156 σ_x^2 are its expected mean value and variance, respectively:

$$PDF: p_\beta(x) = \frac{\Gamma(t)}{\Gamma(r)\Gamma(t-r)} \frac{(x-a)^{r-1}(b-x)^{t-r-1}}{(b-a)^{t-1}}; \quad a \leq x \leq b \quad (4)$$

$$CDF: p_\beta(x) = \int_a^x p_\beta(y) dy \quad (5)$$

157 Where $\Gamma(k)$ is the gamma function of the k -th variable and parameters a , b are assumed
 158 respectively equal to 0 and 6 (Giovinazzi 2005). Parameters t and r are evaluated using Eqs. 6
 159 and 7 (Giovinazzi 2005):

$$t = \frac{\mu_x(a + b - \mu_x) - ab}{\sigma_x^2} - 1 \quad (6)$$

$$r = t \frac{\mu_x - a}{b - a} \quad (7)$$

But t is usually assumed constant and equal to 8 (see Bernardini et al. 2007).

160 The beta probability distribution function is used to obtain discrete probability distributions
 161 associated to every damage level, D_k , as shown by Eq. 8:

$$P(D_k) = \int_k^{k+1} p_\beta(x) dx \quad ; \quad k = 1 \div 5 \quad (8)$$

162 Where $P(D_k)$ the probability of the building to suffer a damage level D_k , with k in the $[0 \div 5]$
 163 range.

164 Expected losses are particularly relevant due to the high fragility of the built environment
 165 (D'Ayala et al., 1997). Their evaluation is performed considering both economic and human
 166 losses. Economic losses are usually divided between direct and indirect losses. For example,
 167 direct losses may refer to the physical damage undergone by a building, while indirect losses
 168 may refer to the income lost by the commercial activity carried on in the damaged building.
 169 Human losses are usually divided in casualties, injured and homelessness. To estimate expected
 170 losses, the exposure of the building, i.e. its social and economic value has to be assigned.

171 Due to the multiple factors that take part in the risk definition (see Eq. 1) seismic
 172 evaluations of single buildings can be extremely challenging and time consuming, but the
 173 evaluation complexity further increases when passing to the urban scale. In fact, to properly
 174 assess the risk of urban systems it is necessary to take into account additional factors, such as
 175 the buildings' functions and their interconnections. For this reason, prevention planning and

176 urban management should consider at first that the overall vulnerability of a city is not the mere
177 sum of the single buildings' vulnerabilities. Furthermore, the overall scope of risk management
178 and reduction should be to increase resilience, defined as "the ability of social units to mitigate
179 hazards, containing the effect of disasters when they occur and carry out recovery activities in
180 the shortest time possible" (Bruneau et al. 2003).

181 The resilience definition is the result of socio-economic considerations, and can be
182 framed in a more comprehensive approach to risk assessment and management, using
183 performance concepts of modern structural design philosophies, such as the Performance Based
184 Earthquake Engineering or PBEE (SEAOC 1995; Staniscia, Spacone and Fabietti 2017). PBEE
185 is based on the definition of performance levels and is quite an effective approach in dealing
186 with risk at the single structure level. For different hazard levels, minimum performance levels
187 (or limit states) are defined for the structural system at hand. In analogy to what is done for
188 structures, different performance levels or *limit conditions for urban settlements*, have been
189 proposed (Olivieri et al. 2011). Table III shows five different performance levels, whose
190 definition is based on the minimum response requested to the city's elements.

191 Among the different performance levels, the *Emergency Limit Condition* (ELC) is
192 introduced as the settlement's extreme capacity, where full functionality is required of only
193 those elements (buildings, connection routes and relative infrastructures) needed during the
194 emergency phase. The ELC cannot be strictly considered as a "urban limit condition", given
195 that the settlement safeguarding and recovery are not guaranteed. The ELC analysis for urban
196 settlements was recently introduced by the Italian Civil Protection Department in an effort to
197 enhance emergency preparedness in the case of an earthquake with catastrophic consequences
198 (Bramerini et al. 2014). It represents a first step towards the definition of a complete
199 performance-based approach to urban risk management.

200 These concepts have a great potential to give new impulse to urban risk management.
201 However they have only been applied to a few case studies and their validity is yet to be fully
202 shown. It is a main goal of this work to propose an effective procedure for the urban seismic
203 risk assessment and management, based on performance concepts and on mechanically proper
204 model of the urban system within reliability framework. Therefore, the “robustness” of the city
205 is evaluated, identifying primarily those elements that have a higher or strategic role in the city
206 life (hospitals, public buildings, fire stations, main connections, etc.). The seismic risk
207 assessment at the urban scale is then performed using a semi-automated procedure, with the
208 single buildings’ vulnerabilities as input data.

209 Section 2 of the present work introduces the proposed methodology and highlights the
210 authors’ original contributions. Section 3 presents the implemented evaluation process, carried
211 out with a MATLAB[®] script. For sake of clarity, the methodology steps are summarized in a
212 flowchart. Section 4 presents the application of the proposed procedure to a case study, the ELC
213 sub-system of Concordia sulla Secchia, Italy. This city was hit by the PPE in 2012, and it is
214 used here as a case study to compare the observed post-seismic damages to the loss scenario
215 predicted by the proposed methodology. Section 5 summarizes the paper’s key points, draws
216 the conclusions and points to future research directions.

217 **2. PROPOSED METHODOLOGY FOR THE SEISMIC RISK ASSESSMENT OF** 218 **HISTORICAL CITY CENTERS**

219 In this paper, a combined approach of the *Vulnerability Index* and the *Macroseismic*
220 *method* is adopted. This approach has been recently applied in seismic risk assessments of
221 historical city centres in Portugal (Vicente et al. 2011; Ferreira et al. 2013; Maio et al. 2016)
222 even though it is limited to unreinforced masonry buildings (URMs). Following this approach,
223 the definition of buildings vulnerability is performed using the Vulnerability Index method, by
224 determining I_V values for each element under assessment. In the same way, the definition of

225 buildings damage is performed using the Macroseismic method, by determining V values. For
226 this reason, a correlation between parameters I_V and V is required. In this work, the formulation
227 proposed by Ferreira et al. (2013) is assumed for vulnerability evaluation of masonry buildings,
228 following Eq. 9:

$$V = 0.592 + 0.0057 \cdot I_V \quad (9)$$

229 Then, mean damage grade, μ_D , and discrete probability distributions, $P(D_k)$, for all buildings
230 are evaluated using Eqs. 2 - 8.

231 In the current work, the abovementioned methodology is further developed proposing
232 some original contributions. Specifically, a $I_V - V$ correlation to estimate the damage for RC
233 buildings is derived, a tool for the city multidirectional assessment using the vulnerability
234 ellipse approach is discussed, and the concept of the *urban system survival probability* is
235 introduced and applied on a case study. The main aim is to introduce a performance-based
236 approach to the seismic risk assessment, as well as to make the methodology usable also for
237 other structural typologies. All contributions are described in detail in the following paragraphs.

238 **2.1 Urban system survival probability**

239 Assessing the seismic risk at the urban scale implies dealing with a large number of
240 elements and their associated damage levels and probabilities. In a city, different constructions
241 have different roles, making them more or less relevant for the city life. Roads, bridges, water
242 supply, electric distribution and ICT networks are also part of the urban system and a complete
243 damage scenario would have to include all of them along with their interdependencies to
244 accurately assess the earthquake impact (see Pederson et al. 2006). However, because of the
245 task complexity and the limitation of available data, the present pilot study considers only
246 buildings and connections, letting to future developments the inclusion of other elements. Even
247 with this limitation, the behaviour of the city can still be well represented, particularly by
248 considering the ELC sub-system described in the previous chapter.

249 The city can be seen as a complex system of interconnected components. The easiest
 250 method to describe such a system is to model it making use of *series* or *parallel* elements
 251 configurations (Pinto, Giannini and Franchin 2007). In a *series* configuration of n elements, if
 252 the single e -th component fails, the entire system fails. It can be associated with the “weakest-
 253 link” concept. In a *parallel* configuration of n elements, if the single e -th component survives,
 254 the entire system survives. It can be associated with the “fail-safe” concept.

255 Given the failure probability of the e -th component, P_e , under the assumption that the
 256 elements’ failures and survivals are independent, the probability of survival of the series
 257 systems, P_S , and parallel systems, P_P , can be expressed by the Eqs. 10 and 11, respectively
 258 (Pinto, Giannini and Franchin 2007):

$$P_S[\textit{survival}] = 1 - P_S[\textit{failure}] = \prod_{e=1}^n (1 - P_e) \quad (10)$$

$$P_P[\textit{survival}] = 1 - P_P[\textit{failure}] = 1 - \prod_{e=1}^n P_e \quad (11)$$

259 Series and parallel systems can be combined together in a *parallel-series system*
 260 configuration. In this configuration, m components are arranged in n parallel sub-systems that
 261 are connected in series. Given the failure probability of the j -th element in the e -th sub-
 262 system, P_{ej} , the probability of survival of the parallel-series systems, P_{PS} , can be expressed by
 263 Eq. 12:

$$P_{PS}[\textit{survival}] = 1 - P_{PS}[\textit{failure}] = \prod_{e=1}^n \left(1 - \prod_{j=1}^m P_{ej} \right) \quad (12)$$

264 The Macroseismic method (Lagomarsino and Giovinazzi, 2006) described in §1 returns the
 265 probability $P(D_k)$ that the e -th building suffers a given damage level, D_k . A specific damage
 266 threshold, D_{max} , can be defined for the e -th building, depending on its function in the city-life.
 267 In this way, if the e -th building under assessment suffers a damage level $D_k \geq D_{max}$, the
 268 building is considered to be failed. For this reason, the failure probability of the e -th building

269 $P_e = P(D_k \geq D_{max})$. Then, the overall urban system survival probability is computed by
 270 combining the failure probabilities P_e through Eqs. 10 - 12, depending on the selected system
 271 configurations of series-parallel systems, which represent different urban performance levels
 272 of Table III. The procedure is herein described in detail.

273 **ELC** – The *emergency sub-system* of the city is considered, formed by the essential
 274 elements for carrying out emergency operations. Very few strategic buildings are included,
 275 together with the main roads connecting them and the open spaces where people can gather.
 276 Strategic buildings and connection routes are identified by the Municipal Authorities and Civil
 277 Protection Departments, as they play a relevant role in the emergency phase. The emergency
 278 sub-system also includes *interfering* buildings, whose collapse can interrupt main
 279 communication roads and cause significant delays to emergency operations. Buildings not
 280 included in the ELC can undergo even severe damage. The ELC is well represented by a *series*
 281 *system* configuration (Fig. 2), where its E_e -th component belongs to the *emergency sub-system*
 282 of the city. As the ELC is the minimum performance level of the city (Olivieri et al., 2011) only
 283 the *main* strategic buildings are taken into account, leaving aside the *redundant* strategic
 284 buildings. In this framework, a strategic building is considered redundant when it is not essential
 285 in the emergency phase. The assumed definition of main and redundant strategic building is
 286 derived by Civil Protection Department Guidelines (Bramerini et al., 2014). The survival
 287 probability of the urban system is evaluated using Eq. 10. Failure probability P_e is a function of
 288 maximum admissible damage D_{max} , defined by Eq. 13:

$$\begin{aligned} \text{strategic buildings} \quad P_e &= P(D \geq D_2) \\ \text{interfering buildings} \quad P_e &= P(D \geq D_4) \end{aligned} \tag{13}$$

289 where D_4 and D_2 are maximum admissible damage levels corresponding to damage mean
 290 grades $\mu_D = 4$ and $\mu_D = 2$, respectively.

291 **CLC** – The ELC is considered along with redundancies. Similarly to the ELC, the city is
292 assumed to undergo massive damage and interruption of the majority of functions. Still, the
293 addition of redundant strategic buildings increase the robustness of the city towards the seismic
294 event. In this case, the behavior of the city is well represented by a *parallel-series* system, as
295 schematically shown in Fig. 2. The survival probability of the urban system is evaluated using
296 Eq. 12. For strategic and interfering buildings, P_e and D_{max} are defined by Eq. 13.

297 **LSLC** – The CLC is considered along with *critical* constructions, whose function may
298 have a relevant impact on the urban system. Main industrial and commercial facilities, chemical
299 factories or high-density residential buildings are some examples of this category. Their
300 collapse or even interruption of use can cause significant loss in terms of economy and
301 population. The choice of critical buildings to be included in the LSLC is a
302 social/economical/political choice that must be made at the political/administrative level. The
303 behavior of the city is well represented by adding a parallel-series system of c_i elements to the
304 CLC, as schematically represented in Fig. 2. The city is assumed to undergo only modest-to-
305 long interruption of ordinary urban functions. The survival probability of the urban system is
306 evaluated using Eq. 12. For strategic and interfering buildings, P_e and D_{max} are defined by Eq.
307 13. For critical buildings, P_e and D_{max} are defined by Eq. 14:

$$\text{critical buildings } P_e = P(D \geq D_3) \quad (14)$$

308 Where D_3 is the maximum admissible damage level corresponding to damage mean grade $\mu_D =$
309 3.

310 **DLC** – The LSLC is considered along with *ordinary* constructions, which don't have a
311 relevant role in the city-life. The city is assumed to undergo a limited level of damage so that it
312 will be able to recover its original functionality in a short period of time. The majority of
313 residential buildings are included in this category. Similarly to the LSLC, only short-to-modest
314 or partial interruptions of ordinary urban functions are accepted. The behaviour of the city is

315 well represented by adding a parallel-series system of o_k elements to the LSLC, as
 316 schematically represented in Fig. 2. The survival probability of the urban system is evaluated
 317 using Eq. 12. A lower maximum damage level D_{max} is requested for all buildings, including
 318 strategic and interfering elements, in order to guarantee the shortest recovery time for the city.
 319 For all buildings, P_e and D_{max} are defined by Eq. 15:

$$\begin{aligned}
 \textit{strategic buildings} \quad P_e &= P(D \geq D_1) \\
 \textit{interfering buildings} \quad P_e &= P(D \geq D_3) \\
 \textit{critical buildings} \quad P_e &= P(D \geq D_2) \\
 \textit{ordinary buildings} \quad P_e &= P(D \geq D_3)
 \end{aligned}
 \tag{15}$$

320 Where D_3 , D_2 and D_1 are the damage levels referred to the damage mean grade $\mu_D = 3$, $\mu_D =$
 321 2 and $\mu_D = 1$, respectively.

322 **OLC** – Conceptually similar to the DLC, see Fig. 2, strategic and critical buildings do not
 323 have to undergo any interruption of use and only low damage of ordinary urban functions is
 324 accepted. This limit condition represent the ideal situation where the system is able to withstand
 325 the seismic event without losing its original functionality. The survival probability of the urban
 326 system is evaluated using Eq. 12. A lower maximum damage level D_{max} than the DLC is
 327 requested for all buildings. For all buildings, P_e and D_{max} are defined by Eq. 16:

$$\begin{aligned}
 \textit{strategic buildings} \quad P_e &= P(D \geq D_0) \\
 \textit{interfering buildings} \quad P_e &= P(D \geq D_2) \\
 \textit{critical buildings} \quad P_e &= P(D \geq D_1) \\
 \textit{ordinary buildings} \quad P_e &= P(D \geq D_2)
 \end{aligned}
 \tag{16}$$

328 where D_2 , D_1 and D_0 are the damage levels referred to the damage mean grade $\mu_D = 2$, $\mu_D =$
 329 1 and $\mu_D = 0$, respectively.

330 Definitions reported above represent a first attempt to include urban planning concepts in
 331 seismic risk assessment. Of course, infrastructures such as transportation systems (roads,

332 bridges, railways, etc.) or lifelines have to be included in future developments. A more
333 comprehensive and life-like scenario can be evaluated using GIS-based software and modelling
334 the interdependencies of such elements with appropriate models. An interesting example is
335 represented by the *dependency matrix* of the SYNER-G (2011) approach.

336 **2.2 Vulnerability Index extension for masonry aggregates**

337 Masonry buildings in historical city centres are often built in aggregate sequence. It is
338 generally challenging to understand if two contiguous buildings can be considered separately.
339 In fact, seismic risk assessment requires to take into account possible interactions between
340 adjacent buildings even if they are independent from the structural point of view. A simple
341 methodological approach to account aggregate's effects has been proposed by Formisano et al.
342 (2010), providing additional parameters P12-P16 to the vulnerability index, I_v , evaluation given
343 in Table I. In this work, the aforementioned approach is adopted after a thoughtful parameters'
344 recalibration. As a matter of fact, following the original approach, and considering moderate or
345 low vulnerability buildings, the original parameters bring in some cases to negative I_v whereas,
346 by definition, I_v has to be in the range [0-100]. For this reason, scores and weights have been
347 adjusted in order to have non-negative values while keeping as much as possible a similarity
348 with the original method. In the revised version, the additional parameters P12-P16 are
349 modified as reported in Table IV.

350 The introduction of parameters P12-P16 results in a I_v variation of maximum $\pm 30\%$
351 compared to the buildings considered as isolated, and the damage prediction is consequently
352 influenced. The additional parameters have proved to provide better adhesion to the real damage
353 observations of masonry structures.

354 **2.3 $I_v - V$ correlation for RC buildings**

355 The combined *Vulnerability Index - Macroseismic* approach (Vicente et al. 2011; Ferreira
356 et al. 2013; Maio et al. 2016) considers at this stage masonry buildings only. Historical city

357 centers, however, often present a heterogeneous mix of ancient masonry buildings and
358 contemporary RC constructions, mainly due to post-war reconstruction. Vulnerability
359 assessment of these RC buildings is necessary for a complete assessment of possible seismic
360 damage scenarios. A mathematical correlation between the Vulnerability Index I_V and the
361 Vulnerability Parameter V for RC buildings is herein proposed by Eq. 17:

$$V = 0.24 + 0.0165 \cdot I_V - 0.00003333 \cdot I_V^2 \quad (17)$$

362 This correlation represents an update of a previous formulation (Basaglia et al., 2016);
363 specifically, the vulnerability definition of RC has changed, passing from the one defined by
364 CETE Méditerranée (2008) to the original GNDT method (GNDT-SSN, 1994). The reason is
365 due to the weight and scores of the vulnerability parameters that are considered to be
366 overestimated by the first formulation. The above reported Eq. 17 has been derived following
367 the analytical approach proposed by Vicente et al. (2011), and the main steps are briefly
368 summarized below:

- 370 a) According to the classification proposed by Grünthal et al. (1998), RC buildings are most
371 likely defined by vulnerability classes C, E and D;
- 372 b) For these classes, Bernardini et al. (2007) defined the Vulnerability Parameter, V , and the
373 mean damage grade relation $\mu_D = \mu_D(V, I_{EMS-98})$, see Eq. 2;
- 374 c) Using the approach defined by Grimaz (1997) and then FEMA (2015), it is possible to
375 define a mean damage grade relation $\mu_D = \mu_D(I_V, I_{EMS-98})$, where I_V is the vulnerability
376 index;
- 377 d) Mean damage grade relations of steps (b) and (c) are used together to derive the V - I_V
378 relationship given by Eq.14.

379 **2.4 Multidirectional urban risk assessment**

380 Ancient buildings often have an irregular in-plan layout and present different structural
381 properties in different directions. Following the approach proposed by Grimaz (1993) for

382 masonry buildings, structural vulnerability can be considered as the sum of *isotropic* and
383 *anisotropic* factors. The isotropic factor considers all features unrelated to the input direction,
384 such as the building materials' properties and age. The anisotropic factor includes all features
385 dependant on the input direction, such as structural strength and stiffness as well as boundary
386 conditions. It has been proved that directionality of incoming seismic waves along with the
387 building orientation definitely affect the building seismic response. As a consequence, the
388 overall urban vulnerability can be affected by the direction of incoming earthquakes.

389 Building's vulnerability typically assume its maximum value in one direction and its
390 minimum value in the orthogonal direction, and can be effectively described by an elliptical
391 function of the in-plan orientation. The *vulnerability ellipse concept* was firstly introduced by
392 Grimaz (1993, 1997) and applied by Basaglia et al. (2016) to define the Vulnerability Index of
393 buildings along their two principal directions (Fig. 3). This effect is accounted by modifying
394 the Conventional Strength of the GNDT form (Parameter 3) according to Figs. 4a and 4b for
395 masonry and RC buildings respectively.

396 The results obtained by Basaglia et al. (2016), however, have shown that seismic risk
397 assessment results are not much affected by the adoption of the 2D formulation. In order to
398 fully understand this evidence, some different aspects have to be considered. First of all, to date
399 just one out of 11 parameters of the GNDT form (of 16 parameters if the aggregate sequence is
400 taken into account) can be directly defined according to direction. Furthermore, constructions
401 often present different structural deficiencies in both main directions, so that the resulting
402 Vulnerability Indexes may be comparable. Finally, buildings of historical city centers are often
403 arranged according to different orientations, due to the natural growth of the city through time
404 (Fig. 1). For this reason, passing from the single element to the urban scale, the effect of
405 vulnerability's ellipses in various directions may result attenuated.

406 Indeed, this aspect may be highly relevant when dealing with urban systems that have a
407 regular buildings' disposition, where a higher difference in the overall seismic response is found
408 depending on the earthquake's direction of propagation. Additional studies are required in order
409 to properly assess the influence of the vulnerability ellipses on the seismic risk assessment.

410 3. COMPUTER-AIDED RISK ASSESSMENT

411 The proposed methodology for seismic risk assessment at the urban scale has been
412 implemented in a MATLAB® environment. The main steps of the proposed numerical
413 procedure are input data collection, numerical elaboration and GIS graphical visualization. The
414 overall numerical procedure is summarized in the flowchart of Fig. 5.

415 The input data consists of information on buildings and site-effects of the area under
416 consideration. More specifically, for each building, the following parameters are needed:

- 417 • Vulnerability Index I_V is evaluated in both principal directions (see § 1); for masonry and
418 pre-code RC buildings I_V is evaluated by using Tables I and II respectively, for masonry
419 aggregates using Table IV. It is reasonable to assume that all buildings designed according
420 to new generation seismic codes present the lowest vulnerability level, $I_V = 0$.
- 421 • Structure Identifier is assigned to each building: ID = 0 for masonry buildings, ID = 1 for
422 RC buildings and ID = 2 for buildings designed according to modern design codes;
- 423 • Local Soil Amplification Factor, F_a (Power, Borchardt and Stewart 2004), is evaluated from
424 geotechnical test of the considered site. In the case-study presented in §4, amplification
425 factors are derived from tables of the Emilia Romagna region, published in the Public Act
426 DAL 112/2007 (Emilia-Romagna Region 2007).

427 During the assessment, indexes I_V are converted into vulnerability values V according to
428 Eqs. 9 and 17 for masonry (ID = 0) and RC buildings (ID = 1), respectively. For buildings
429 designed according to modern seismic codes, $V = 0.24$ is assigned (Bernardini et al. 2007).
430 Potential seismic site effects of the area under assessment are considered introducing an

431 additional Vulnerability Modifier ΔV , see Eqs. 18 – 20, as proposed by Giovinazzi and
432 Lagomarsino (2004):

$$\bar{V} = V + \Delta V \quad (18)$$

$$\Delta V = \frac{\Delta I}{6.25} \quad (19)$$

433 where:

$$\Delta I = \frac{\ln(F_a)}{0.602} \quad (20)$$

434 and F_a is the local soil amplification factor previously defined.

435 Mean damage grades μ_D are evaluated using Eqs. 2 and 3 for increasing intensities I_{EMS-98}
436 in the [5, 12] range. Lower intensities are not considered as they have negligible impact on
437 buildings. For masonry and RC buildings of the Concordia sulla Secchia ELC, the ductility
438 factor, Q , is assumed equal to 2.3 and 3, respectively. Using the mean damage grades, μ_D ,
439 damage probabilities $P(D_k)$ are defined using Eqs. 4 - 8. Finally, damage distributions are
440 represented using fragility curves.

441 Damage probabilities $P(D_k)$ of all buildings are finally combined to determine the survival
442 probability of the urban system, using models introduced in §2.1 for the considered limit
443 condition (ELC, CLC, LSLC, DLC or OLC). The system survival probability is evaluated for
444 increasing intensities I_{EMS-98} in the [5, 12] range. In this way it is possible to predict the change
445 in the city response towards moderate to strong earthquakes. Damage probabilities $P(D_k)$ can
446 also be used to perform loss evaluations, predicting the number of damaged or unusable
447 buildings as well as the number of casualties and severe injuries or homeless using the equations
448 proposed by Vicente et al. (2011).

449 **4. ELC RISK ASSESSMENT OF CONCORDIA SULLA SECCHIA. CASE STUDY**

450 Comparing actual observed damage with predicted damage scenarios is the only way to
451 improve the accuracy of seismic risk assessment methods. Italy represents a valuable asset in
452 this regard, because of its considerable amount of post-seismic data collections, starting from
453 the early years of the 20th century. For example D'Ayala and Paganoni (2010) have recently
454 used damage data caused by the 2009 L'Aquila earthquake to test the reliability of the FaMIVE
455 method. In that case however, the assessment focused mainly on old typical constructions of
456 the L'Aquila's area, made of stones, bricks and rubbles, while RC buildings were excluded.

457 With a similar approach, in this work the case of the Italian city center of Concordia sulla
458 Secchia has been considered to validate the proposed assessment methodology. Among all the
459 cities hit by the Italian PPE in 2012, Concordia sulla Secchia has been selected due to its
460 peculiar historical city center, made of a heterogeneous mix of masonry and RC buildings that
461 date back to different periods of time and are typically built in aggregate sequence. After the
462 PPE occurred, the Municipal authorities of Concordia commissioned a post-earthquake survey
463 to the University of Ferrara (Regione Emilia-Romagna 2013), hanks to which geometrical and
464 structural features of all buildings were gathered.

465 The PPE occurred on May 20, 2012 at 4:03 pm was classified of Magnitude Richter 5.9 (\pm
466 0.3) by the Italian National Institute of Geology and Volcanology (INGV). The epicentre was
467 located at 8 km NW from Finale Emilia city with coordinates 44.89 ° N - 11.23 ° E and 6.3 km
468 depth. The predominant incoming direction of PPE was WNW - ESE or 22° East. The
469 municipalities closest to the epicentre were located on the border of Modena, Ferrara, Rovigo
470 and Mantova provinces. Based on the National Seismic Network data, the shake map of the
471 event was determined by INGV in an area of approximately 30x30 km² around the epicentre.
472 Fig. 6 put in evidence that Concordia sulla Secchia experienced I_{EMS-98} in the [7, 8] range.

473 The ELC sub-system was defined by the Municipal Authorities of Concordia jointly with
474 the Italian Civil Protection Department. Based on strategic buildings location and connecting
475 main roads, the ELC sub-system is composed by a total of 42 elements: 4 strategic buildings
476 (hosting a Day Care, a Kindergarten to Secondary School Institute, the City Hall and a Sports
477 Centre) and 38 interfering buildings (hosting residential and commercial activities). From the
478 structural point of view, 1 out of 4 strategic buildings is a pre-seismic code RC building, while
479 3 out of 4 are recent constructions, built following earthquake engineering design rules; 8 out
480 of 38 interfering buildings are URM buildings built in aggregate sequence and 30 out of 38 are
481 pre-seismic code RC buildings, whose 24 out of 30 are built in aggregate sequence. The ELC
482 sub-system plan of Concordia sulla Secchia is reported in Fig. 7.

483 Thanks to available information, the risk assessment proposed methodology has been
484 applied to the ELC sub-system of Concordia, damage scenarios and related μ_D have been
485 obtained for the PPE event. Finally, the predicted damage scenarios have to be compared with
486 the observed ones. Since the post-earthquake damage survey provides qualitative damage levels
487 through a short description, in order to compare it with the numerical damage assessment, the
488 following equivalence is assumed:

- 489 ▪ *None* damage is related to μ_D in the [0, 1] range;
- 490 ▪ *Very Light* to *Light* damage is related to μ_D in the [1, 2] range;
- 491 ▪ *Moderate* to *Heavy* damage is related to μ_D in the [2, 4] range;
- 492 ▪ *Very Heavy* damage is related to μ_D in the [4, 5] range;

493 The full comparison between observed and predicted damage levels is shown in Table V.
494 Because the earthquake intensity I_{EMS-98} falls in the [7, 8] range, the predicted damage was
495 computed for both intensity levels. For all the assessed buildings, Table V reports a feature
496 identifier FID (used to identify buildings in the map), the vulnerability index I_V in the
497 earthquake incoming direction, the construction period, the structural type, the predicted and

498 observed damage levels. In particular, FID 113, 111, 110 and 112 refer to the 4 strategic
499 buildings described above, respectively. The last columns report the difference $\Delta\mu_D$, between
500 the predicted and the closest observed damage levels.

501 The comparison between damage levels reported in Table V shows that, for $I_{EMS-98} = 7$
502 the predicted damage matches the observed damage in 21 out of 42 buildings (highlighted in
503 bold text and light grey background), with a positive feedback in 50% of cases. For $I_{EMS-98} =$
504 8, the predicted damage matches the observed damage in 26 of the 42 buildings (highlighted in
505 bold text), with a positive feedback in about 62% of cases.

506 Figs. 8 show the frequency distributions of damage difference, $\Delta\mu_D$, where the and value
507 “0” means the matching between predicted and observed post-earthquake damage scenario. For
508 $I_{EMS-98} = 7$ (Fig. 8a) the risk assessment methodology generally underestimates damage, with
509 a deviation of $-0,8 \mu_D$ that, related to the maximum damage grade ($\mu_{D,max} = 5$), means an error
510 of -16%. For $I_{EMS-98} = 8$ (Fig. 8b) the risk assessment methodology generally overestimates
511 damage, with a deviation of $0,6 \mu_D$ and a maximum error of +12%.

512 The performed comparison shows that the damage prediction offered by the proposed
513 methodology is quite reliable. In fact, the results obtained for I_{EMS-98} in the [7, 8] range are
514 generally in good agreement with the post-earthquake survey data. In some cases the predicted
515 and the observed damage are inconsistent (see for example FID 73 or FID 66 - 2). The deviation
516 of the damage predictions may be due to imperfections of the proposed methodology and/or to
517 approximations in the post-earthquake surveys, which were necessarily quick and coarse. This
518 case study represents the first application of the proposed risk assessment methodology and, of
519 course, further validation is deemed essential to test and increase its effectiveness.

520 The ELC sub-system survival probability is represented in Fig. 9. It is obtained by
521 evaluating the probability of single buildings using Eq. 10 and then the overall survival
522 probability using Eq. 7. In fact, by definition of the ELC, all elements are considered to be

523 represented by a series system. It is observed that, for intensity $I_{EMS-98} \geq 7$ the survival
524 probability drops to zero. This means that at least one strategic building or one interfering
525 building has exceeded the considered damage thresholds of Eq. 13, consistently with the series
526 system definition. As the 2012 PPE intensity I_{EMS-98} was in the [7, 8] range, the ELC of
527 Concordia city needs definitely major improvements in order to survive future earthquakes.

528 Assessment output values can be depicted on a city map, as reported in Figs. 10, using the
529 geospatial processing program ArcMap, of the Esri's ArcGIS suite (Chang 2006). Thanks to
530 this suite it is possible to visualize the earthquake effects for different directions and increasing
531 seismic intensities (Cova, 1999). A FID is assigned to each building in order to correctly
532 reference the corresponding output results. Different colour maps can be used to represent the
533 effects of increasing seismic intensities, and to identify the most vulnerable areas.

534 **5. SUMMARY AND CONCLUSIONS**

535 Seismic risk prevention is a urgent global goal that aims at reducing human casualties and
536 economic losses and at preserving the inestimable cultural heritage of historical city centres.
537 This paper proposes a general seismic risk assessment methodology at the urban scale, based
538 on predefined performance level. It can be a useful tool to develop urban risk mitigation plans.
539 The original contributions of the proposed methodology are:

- 540 ■ Performance-based approach has been applied to the urban settlement, resulting in the
541 definition of the urban system survival probability. Thanks to this concept, predicted
542 damages of many structures are used to define a single parameter representing the
543 performance of the whole system, that is easier to understand;
- 544 ■ Masonry constructions built in aggregate sequence are taken into account by updating an
545 existing method. Including this aspect leads to a better estimation of the damage that
546 adheres more to real post-earthquake observations;

- 547 ▪ RC buildings are included in the assessment evaluation. Existing formulations were
548 available only for masonry structures. However, RC buildings constitute a significant part
549 of historical city centres as well, and have to be included in the assessment in order to
550 evaluate the seismic risk at the urban level;
- 551 ▪ Vulnerability ellipse concept has been discussed and implemented in order to obtain the
552 multi-directional assessment of the building performance. It is well know that structural
553 response can be strongly dependent on earthquake direction. At global level, directional
554 assessment is pivotal to produce reliable damage scenarios and related mitigation plans.

555 The proposed assessment method has been implemented in a computer-aided procedure
556 using the MATLAB® software. The output results can be easily visualized by means of simple
557 curves and GIS maps. The proposed automated procedure has been applied to a case study, the
558 historical city centre of Concordia sulla Secchia (Italy), selected for its heterogeneous mix of
559 masonry and RC structures, built in different periods, often in aggregate sequences. The
560 settlement experienced the PPE in 2012, and was object of post-seismic damage survey. The
561 proposed methodology has been carried out on the city ELC sub-system constituted by 42
562 buildings. From the comparison between predicted and observed damage, a matching rate of
563 50% ($I_{EMS-98} = 7$) and 62% ($I_{EMS-98} = 8$) has been found. This latter intensity may be
564 considered as the most representative of the occurred seismic event. Recognizing the
565 complexity of seismic risk assessment at the urban scale, the obtained results are considered
566 promising. However, the procedure needs further validations on more case studies to be
567 improved. Currently, the proposed methodology has been used to assess the expected
568 earthquake damage on the historical Eixample district of Barcelona, Spain (Cara et al. 2018).

569 This paper is part of an ongoing research: the methodology used to estimate damage for
570 the ELC sub-system of Concordia sulla Secchia is being used to assess the positive effects of
571 mitigation strategies, including seismic retrofits. Indeed, expert committees instituted by the

572 regional authorities of Emilia Romagna Region are actually processing post-earthquake
573 reconstruction data in order to assess economic and social consequences produced by the
574 aftermath of PPE in 2012. The application of the proposed methodology is proving to be
575 essential helping the Decision-making Authorities in the task of increasing the resilience of
576 historical city-centres.

577 Future work is expected to address the following issues, listed in order of priority:

- 578 ▪ Definition of GNDT forms (parameters, scores and weights) for other structural types (for
579 example precast, mixed structures and steel buildings);
- 580 ▪ Integration of the GNDT forms with the aggregate effect and seismic retrofits;
- 581 ▪ Simplification of the vulnerability assessment of huge urban systems. Large scale analyses
582 require unacceptable time efforts to carry out the detailed survey needed to fill the GNDT
583 (GNDT-SSN 1994) forms for all buildings. Following the Portuguese approach (Vicente et
584 al. 2011; Ferreira et al. 2013; Maio et al. 2016) a “representative sample” should be defined
585 to reasonably estimate the vulnerability of the remaining buildings.
- 586 ▪ Inclusion of infrastructures like bridges, water supply, electric distribution and ICT
587 networks in the urban risk assessment, as they represent the most critical facilities or
588 “backbone” of the overall emergency response and post-event recovery;

589 **ACKNOWLEDGMENTS**

590 This research was partly funded by FAR funding of University of Ferrara, 2015 “Historical
591 Centers Livable and Sustainable (HC-LIVE)” and by the Erasmus+ Program of the University
592 of Ferrara in association with the Trinity College Dublin.

593 The authors wish to acknowledge Profs. Riccardo Dalla Negra, Marco Zuppiroli and Francesco
594 Guidi of the University of Ferrara for providing the survey data of the case study.

595 **REFERENCES**

596 Anagnos T., Rojahn C. and Kiremidjian A. 1995. NCEER-ATC Joint Study on Fragility of
597 Buildings. *National Center for Earthquake Engineering Research: Technical Report*. ISSN
598 1088-3800.

599 Basaglia A., Aprile A., Pilla F. and Spacone E. 2016. Computer-aided risk assessment at urban
600 scale. Model definition and validation on a case study. *ECCOMAS 2016 Congress Proceedings:*
601 Vol. 3, pp. 5977-5986. Hersonissos, Crete Island.

602 Benedetti D. and Petrini V. 1984. Sulla vulnerabilità sismica di edifici in muratura: Un metodo
603 di valutazione. *L'Industria delle Costruzioni*: 149 (18):66-78. Italian.

604 Bernardini A., Giovinazzi S., Lagomarsino S., Parodi S. 2007. The vulnerability assessment of
605 current buildings by a macroseismic approach derived from the EMS-98 scale. *Proceedings of*
606 *the Third National Congress on Earthquake Engineering*, Spanish Association of Earthquake
607 Engineering, Girona, 8-11 May.

608 Bertero V.V. 2000. Performance-based seismic engineering: conventional vs. innovative
609 approaches. In: *Proceedings of the 12WCEE 2000: 12th World Conference on Earthquake*
610 *Engineering*, Auckland, New Zealand, paper no. 2074, 8 pp

611 Bramerini F., Di Pasquale G., Orsini A., Pugliese A., Romeo R. and Sabetta F. 1995. Rischio
612 sismico del territorio italiano. Proposta per una metodologia e risultati preliminari. *Rapporto*
613 *tecnico del Servizio Sismico Nazionale: SSN/RT/95/01*, Roma.

614 Bramerini F., Conte C., Di Pasquale G., Fazio F., Parotto R. and Speranza E. 2014. Manuale
615 per l'analisi della Condizione Limite per l'Emergenza (CLE) dell'insediamento urbano.
616 *BetMultimedia*, Rome. Italian.

617 Bruneau M., Chang E. S., Eguchi R. T., Lee G. C., O'Rourke T. D., Reinhorn A. M., Shinozuka
618 M., Tierney K., Wallace W. A. and von Winterfeldt D. 2003. A Framework to Quantitatively
619 Assess and Enhance the Seismic Resilience of Communities. *Earthquake Spectra*: Vol. 19, No.
620 4, pp. 733-752.

621 Cara S. Aprile A., Pelà L. and Roca P. 2018. Seismic risk assessment and mitigation at
622 Emergency Limit Condition of historical buildings along strategic urban roadways. Application
623 to the "Antiga Esquerra de l'Eixample" neighbourhood of Barcelona. *International Journal of*
624 *Architectural Heritage*. Present Volume.

625 CETE Méditerranée (DREC/SVGC-SIG). 2008. Comparaison de méthodes qualitatives
626 d'évaluation de la vulnérabilité des constructions aux séismes. Plan séisme - action 2.4.7. Guide
627 des méthodes de diagnostics de la résistance des bâtiments aux séismes. *Convention*
628 *MEDD/CETE n°CV05000107*: Étude réalisée dans le cadre des projets de Service public du
629 BRGM. (French).

630 Chang K. T. 2006. Geographic Information System. *John Wiley & Sons*, Ltd.

631 Chopra AK, Goel RK (1999) Capacity-demand-diagram methods based on inelastic design
632 spectrum. *Earthq Spectra* 15(4):637–656.

633 CotEU. Council conclusions of 21 may 2014 on cultural heritage as a strategic resource for a
634 sustainable Europe. 2014. *Official Journal of the European Union*: 57 (C 183):36:8.

635 Cova T. J. 1999. GIS in emergency management, *Geographical Information Systems:*
636 *Principles, Techniques, Applications, and Management*. *Geographical Information Systems:*
637 *Principles, Techniques, Applications, and Management*: Chapter: 60, pp.845-85, John Wiley &
638 Sons.

639 D'Ayala D., Spence R., Carlos O., and Pomonis A. 1997. Earthquake Loss Estimation for
640 Europe's Historic Town Centres, *Earthquake Spectra*: 13 (4):773-793. DOI:
641 10.1193/1.1585980.

642 D'Ayala D. and Paganoni, S. 2010. Assessment and analysis of damage in L'Aquila historic
643 city centre after 6th April 2009. *Bulletin of Earthquake Engineering*: 9 (1):81-104.
644 DOI:10.1007/s10518-010-9224-4.

645 D'Ayala D. and Kishali E. 2012. Analytically derived fragility curves for unreinforced masonry
646 buildings in urban contexts. *15th World Conference of Earthquake Engineering*, Lisbon.

647 Di Mauro G. 2014. I costi dei terremoti in Italia. *Consiglio Nazionale Degli Ingegneri*, Roma.
648 Italian.

649 FEMA. 2015. HAZUS-MH 2.1 Multi-hazard Loss Estimation Methodology User Manual.
650 *Federal Emergency Management Agency*.

651 Ferreira T. M., Vicente R., Mendes Silva J. A. R., Varum H. and Costa A. 2013. Seismic
652 vulnerability assessment of historical urban centres: Case study of the old city centre in Seixal,
653 Portugal. *Bulletin of Earthquake Engineering*: 11 (5):1753-73. DOI: 10.1007/s10518-013-
654 9447-2.

655 Ferreira T. M., Vicente R. and Varum H. 2014. Seismic vulnerability assessment of masonry
656 facade walls: development, application and validation of a new scoring method. *Structural*
657 *Engineering and Mechanics*: 50:541-561. DOI: 10.12989/sem.2014.50.4.541.

658 Formisano A., Mazzolani F. M., Florio G. and Landolfo R. 2010. A quick methodology for
659 seismic vulnerability assessment of historical masonry aggregates. *COST Action C26*, 16-18
660 September, Naples.

661 Gobarah A. 2004. On drift limits associated with different damage levels. *Proceedings of*
662 *International Workshop on Performance-Based Seismic Design*, Department of Civil
663 Engineering, McMaster University, Bled, 28 June-1 July.

664 Giovinazzi S. and Lagomarsino S. 2004. A macroseismic method for the vulnerability
665 assessment of buildings. *13th World Conference on Earthquake Engineering*: Vancouver, B.C.,
666 Canada, August 1-6.

667 Giovinazzi S. 2005. The vulnerability assessment and the damage scenario in seismic risk
668 analysis. PhD Thesis.

669 GNDT-SSN. 1994. Scheda di esposizione e vulnerabilità e di rilevamento danni di primo livello
670 e secondo livello (muratura e cemento armato). *Gruppo Nazionale per la Difesa dai Terremoti*,
671 Roma. (Italian).

672 Grimaz S. 1993. Valutazione della vulnerabilità sismica di edifici in muratura appartenenti ad
673 aggregati strutturali sulla base di analisi a posteriori. *Ingegneria Sismica*: 3:12-22. Italian.

674 Grimaz S., Meroni F., Petrini V., Tomasoni R., Zonno G. 1997. Il ruolo dei dati di
675 danneggiamento del terremoto del Friuli nello studio di modelli di vulnerabilità sismica degli
676 edifici in muratura. In: *La scienza e i terremoti*, Udine: Forum Editore, p. 89- 96, Italian.

677 Grünthal G., Musson R., Schwarz J. and Stucchi, M. 1998. European macroseismic scale.
678 Centre Européen de Géodynamique et de Séismologie, Luxembourg; Vol. 15.

679 Lagomarsino S. and Giovinazzi S. 2006. Macroseismic and mechanical models for the
680 vulnerability and damage assessment of current buildings. *Bulletin of Earthquake Engineering*:
681 4:415–443. DOI 10.1007/s10518-006-9024-z.

682 Lang K., and Bachmann H. 2003. On the seismic vulnerability of existing unreinforced masonry
683 buildings. *Journal of Earthquake Engineering*: 7(3):407-426. DOI:
684 10.1080/13632460309350456.

685 Lantada N., Irizarry J., Barbat A.H., Goula X., Roca A., Susagna T. and Pujades L.G. 2010.
686 Seismic hazard and risk scenarios for Barcelona, Spain, using the Risk-UE vulnerability index
687 method. *Bulletin of Earthquake Engineering*: 8:201–229.

688 Maio R., Ferreira T. M., Vicente R. and Estêvão J. 2016. Seismic vulnerability assessment of
689 historical urban centres: case study of the old city centre of Faro, Portugal. *Journal of Risk*
690 *Research*: 19 (5), DOI: 10.1080/13669877.2014.988285.

691 McGuire R. K. 2004. Seismic hazard and risk analysis. *Earthquake Engineering Research*
692 *Institute*, Oakland.

693 Mouroux P., Bertrand E., Bour M., Le Brun B., Depinois S. and Masure P. 2004. The European
694 Risk-Ue Project: An Advanced Approach To Earthquake Risk Scenarios. *Proceedings of the*
695 *13th World Conference on Earthquake Engineering*: Vancouver, Canada.

696 Olivieri M., Benigni M. S., De Girolamo F., De Rosa A., Di Salvo G., Fazzio F., Fiorito M.,
697 Giuffrè M., Pellegrino P., Parotto R. and Pizzo B. 2011. Rischio sismico urbano: Indicazioni di
698 metodo e sperimentazioni per l'analisi della condizione limite per emergenza e la struttura
699 urbana minima. *Act of 2011*, DGR (Pub. L.) No. 793, Emilia Romagna. Italian.

700 Pederson P., Dudenhoefter D., Hartley S., and Permann M. 2006. Critical Infrastructure
701 Interdependency Modeling: A Survey of U.S. and International Research. *Report INL/EXT-06-*
702 *11464*. Idaho National Laboratory, Idaho Falls, ID.

703 Pinto P.E., Giannini R. and Franchin P. 2007. Seismic reliability analysis of structures. *IUSS*
704 *Press*.

705 Podestà S., Romano C. 2014. A Macro seismic method for vulnerability assessment of
706 Rationalist architectural heritage. *Proceedings of 4th International Conference on Building*
707 *Resilience, Incorporating the 3rd Annual Conference of the ANDROID Disaster Resilience*
708 *Network*, 8th – 11th September 2014, Salford Quays, United Kingdom.

709 Porter K. A. 2003. An Overview of PEER’s Performance-Based Earthquake Engineering
710 Methodology. *Proceeding of the Ninth International Conference on Applications of Statistics*
711 *and Probability in Civil Engineering (ICASP9)*.

712 Porter K. A. 2017. A Beginner’s Guide to Fragility, Vulnerability, and Risk. *Encyclopedia of*
713 *Earthquake Engineering*: pp.235-260, DOI: 10.1007/978-3-642-35344-4_256.

714 Power M., Borchardt R. and Stewart J. 2004. Site amplification factors from empirical studies.
715 *NGA Working Group #5*: Sponsored by the Pacific Earthquake Engineering Research Center,
716 University of California, Berkeley.

717 Regione Emilia-Romagna. 2007. Indirizzi per gli studi di microzonazione sismica in Emilia-
718 Romagna per la pianificazione territoriale e urbanistica. *Delibera Giunta Regionale (Pub. Law)*
719 No. 112-3121. Italian.

720 Regione Emilia-Romagna. 2013. Convenzione tra il Comune di Concordia sulla Secchia e
721 l’Università di Ferrara per il supporto tecnico e scientifico in ordine alle attività di rilevamento
722 e restituzione, propedeutiche all’individuazione ed all’attuazione delle unità minime di
723 intervento (UMI) così come previsto dalla L.R. n°16 del 21 Dicembre 2012 “Norme per la
724 ricostruzione nei territori interessati dal sisma del 20 e 19 maggio 2012”. *Deliberazione*
725 *Consiglio Comunale (Reg. Law) No. 35-219*. Italian.

726 SEAOC. Vision 2000. 1995. Performance-Based Seismic Engineering. Sacramento, California.

727 Staniscia S., Spacone E. and Fabietti V. 2017. Performance based urban planning: Framework
728 and L'Aquila historic city center case study. *International Journal for Architectural Heritage*:
729 pp. 1-14. In press.

730 SYNER-G. 2011. Systemic Seismic Vulnerability and Risk Analysis for Buildings, Lifeline
731 Networks and Infrastructures Safety Gain – D2.1: General methodology for systemic
732 vulnerability assessment. Aristotle University of Thessaloniki.

733 UNISDR. Sendai framework for disaster risk reduction 2015-2030. 2015. *Third UN World*
734 *Conference*: Sendai, Japan.

735 Vicente R., Parodi S., Lagomarsino S., Varum H. and Mendes Silva J. A. R. 2011. Seismic
736 vulnerability and risk assessment: Case study of the historic city centre of Coimbra, Portugal.
737 *Bulletin of Earthquake Engineering*: 9 (4), pp. 1067-96. DOI: 10.1007/s10518-010-9233-3.

738

739

740

741

742

743

744

745

746

747

748

749

750

751 **LIST OF FIGURES**

752 **Fig. 1.** Vulnerability methods at different scales.

753 **Fig. 2.** Schematic representation of ELC, CLC, LSLC, DLC and OLC using series and parallel
754 systems.

755 **Fig. 3.** Vulnerability ellipse concept.

756 **Fig 4.** Modified Conventional Strength (Parameter 3) of the GNDT form for **(a)** masonry
757 buildings; **(b)** RC buildings.

758 **Fig. 5.** Flowchart of the risk assessment procedure.

759 **Fig. 6.** Italian PPE shake map (adapted by INGV) for the Pianura Padana Earthquake of May
760 20, 2012.

761 **Fig. 7.** ELC plan of Concordia sulla Secchia (aerial view and location of assessed buildings).

762 **Fig. 8.** $\Delta\mu_D$ frequency distribution of the Concordia sulla Secchia ELC sub-system for **(a)**
763 $I_{EMS-98} = 7$; **(b)** for $I_{EMS-98} = 8$.

764 **Fig. 9.** Survival probability of the Concordia sulla Secchia ELC sub-system.

765 **Fig. 10.** Damage grade maps of the Concordia sulla Secchia ELC sub-system for **(a)** $I_{EMS-98} =$
766 7 ; **(b)** for $I_{EMS-98} = 8$.

767

768

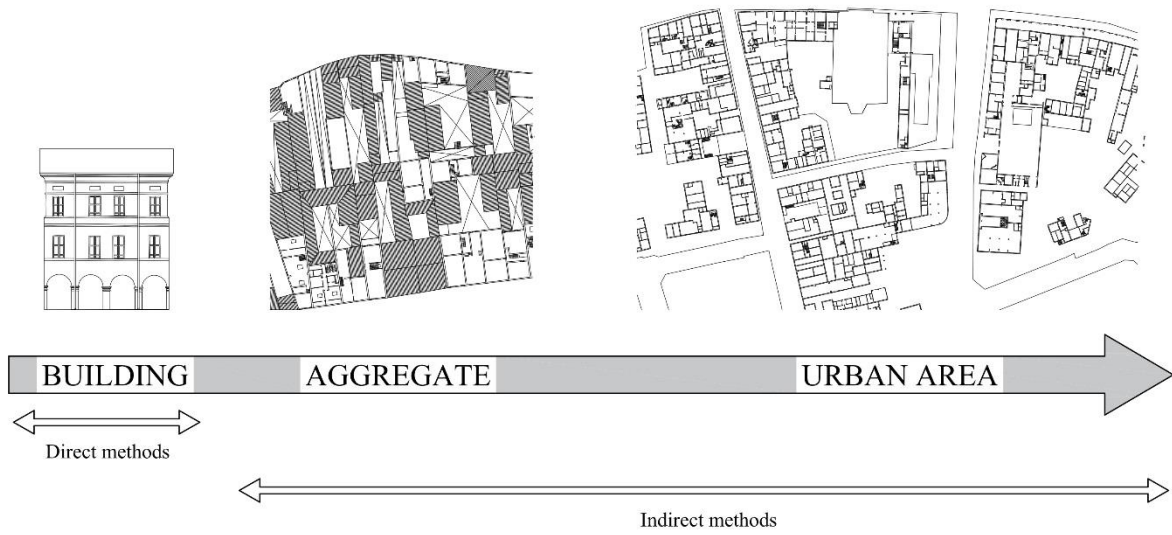
769

770

771

772

773



774

775

Fig. 1. Vulnerability methods at different scales.

776

777

778

779

780

781

782

783

784

785

786

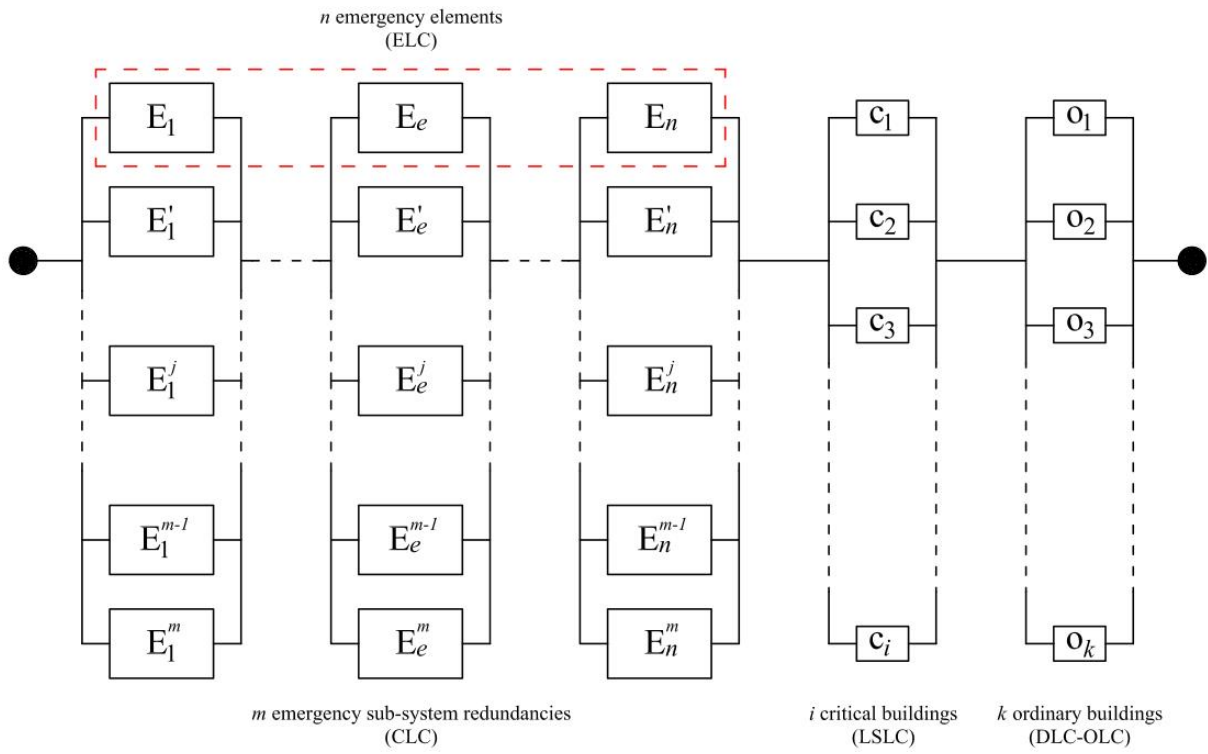
787

788

789

790

791



792

793

Fig. 2. Schematic representation of ELC, CLC, LSLC, DLC and OLC using series and

794

parallel systems.

795

796

797

798

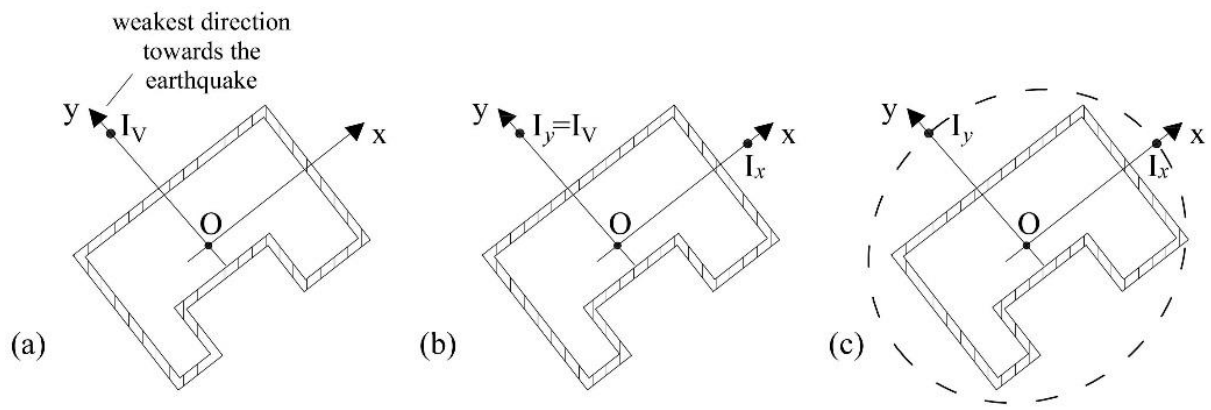
799

800

801

802

803



804

Fig. 3. Vulnerability ellipse concept.

805

806

807

808

809

810

811

812

813

814

815

816

817

818

819

820

821

822

PARAMETER 3 GNDT FORM (Conventional Strength)																													
MASONRY BUILDINGS			R.C. BUILDINGS																										
Building's no. of stories	N	[-]	Building's no. of stories	N	[-]																								
Roof area	A _R	[m ²]	Average interstorey height	h	[m]																								
Resisting area in X-direction	A _X	[m ²]	Total height of building	H	[m]																								
Resisting area in Y-direction	A _Y	[m ²]	Fundamental vibration period	T ₁	[s]																								
Transversal strength reference	k	[t/m ²]	Ground type	(S1 or S2)																									
Average interstorey height	h	[m]	Seismic coefficient	R	[-]																								
Unit weight of brick walls	P _m	[t/m ³]	Total seismic force (ΣF _i *)	FS	[t]																								
Distributed load of ceilings	P _s	[t/m ²]																											
Evaluation in X-direction	a _{0,X}	[-]	REINFORCED CONCRETE	No. of pillars	n _{pil}	[-]																							
	γ	[-]		Average pillar side length	l _{pil}	[m]																							
	q	[t/m ²]		R.C. resistant area	A _{R.C.}	[m ²]																							
	C	[-]		Transv. strength reference	τ _k	[t/m ²]																							
	α _X	[-]		R.C. Young modulus	E _{R.C.}	[t/m ²]																							
Evaluation in Y-direction	a _{0,Y}	[-]	MASONRY (infill walls)	Toral resistant force (A·τ)	FR	[t]																							
	γ	[-]		Alfa coefficient	α	[-]																							
	q	[t/m ²]		Main resistant direction	(X or Y or NONE)																								
	C	[-]		Form coefficient	β	[-]																							
	α _Y	[-]		Masonry class	(A, high or B, low quality)																								
$a_0 = \frac{A}{A_{TOT}}$ $\gamma = \frac{B}{A}$ $q = (A_x + A_y) \cdot h \cdot \left(\frac{P_m}{A_{TOT}} \right)^{1.5} + P_s$ $C = \frac{a_0 \cdot \tau_k}{q \cdot N} \cdot 1 + \left[\frac{q \cdot N}{1.5 \cdot a_0 \cdot \tau_k \cdot (1 + \gamma)} \right]^{0.5}$ $\alpha = \frac{C}{0.4}$ <p>X-direction: A_x = A ; A_y = B Y-direction: A_y = A ; A_x = B</p>	MASONRY	<table border="1"> <tr> <td>T₀</td> <td>r</td> <td>R₀</td> <td>0 < T < T₀, R=R₀</td> </tr> <tr> <td>S1</td> <td>0.35</td> <td>2/3</td> <td>2.6</td> </tr> <tr> <td>S2</td> <td>0.8</td> <td>2/3</td> <td>2.2</td> </tr> </table> <p>T₀ < 0, R = $\frac{R_0}{(T - T_0)^2}$</p> <p>F_i = 0.4 · R · W_i · h_i · $\frac{\sum W_j}{\sum W_j h_j}$ for the i-th floor W_i, floor weight α = A · τ / F_S</p> <table border="1"> <tr> <td>X main res. dir.</td> <td>Y main res. dir.</td> <td>NO main res. dir.</td> </tr> <tr> <td>$\beta = \frac{A_{RC,X} + n \cdot A_{M,X}}{A_{RC,Y} + n \cdot A_{M,Y}}$</td> <td>$\beta = \frac{A_{RC,Y} + n \cdot A_{M,Y}}{A_{RC,X} + n \cdot A_{M,X}}$</td> <td>β = 1</td> </tr> <tr> <td>α_X = β · α</td> <td>α_X = α</td> <td>α_X = α</td> </tr> <tr> <td>α_Y = α</td> <td>α_Y = β · α</td> <td>α_Y = α</td> </tr> </table>	T ₀	r	R ₀	0 < T < T ₀ , R=R ₀	S1	0.35	2/3	2.6	S2	0.8	2/3	2.2	X main res. dir.	Y main res. dir.	NO main res. dir.	$\beta = \frac{A_{RC,X} + n \cdot A_{M,X}}{A_{RC,Y} + n \cdot A_{M,Y}}$	$\beta = \frac{A_{RC,Y} + n \cdot A_{M,Y}}{A_{RC,X} + n \cdot A_{M,X}}$	β = 1	α _X = β · α	α _X = α	α _X = α	α _Y = α	α _Y = β · α	α _Y = α	R.C.	MASONRY (infill walls)	Masonry resistant area in X A _{M,X} [m ²] Masonry resistant area in Y A _{M,Y} [m ²] Transv. strength reference τ _k [t/m ²] Masonry Young modulus E _M [t/m ²] Modular ratio (E _M / E _{R.C.}) n [t] Pillars' no. in X-direction n _{pil,X} [-] Pillars' no. in Y-direction n _{pil,Y} [-]
	T ₀	r	R ₀	0 < T < T ₀ , R=R ₀																									
	S1	0.35	2/3	2.6																									
	S2	0.8	2/3	2.2																									
	X main res. dir.	Y main res. dir.	NO main res. dir.																										
	$\beta = \frac{A_{RC,X} + n \cdot A_{M,X}}{A_{RC,Y} + n \cdot A_{M,Y}}$	$\beta = \frac{A_{RC,Y} + n \cdot A_{M,Y}}{A_{RC,X} + n \cdot A_{M,X}}$	β = 1																										
	α _X = β · α	α _X = α	α _X = α																										
	α _Y = α	α _Y = β · α	α _Y = α																										
				Evaluation in X-direction	α _X	[-]																							
				Evaluation in Y-direction	α _Y	[-]																							

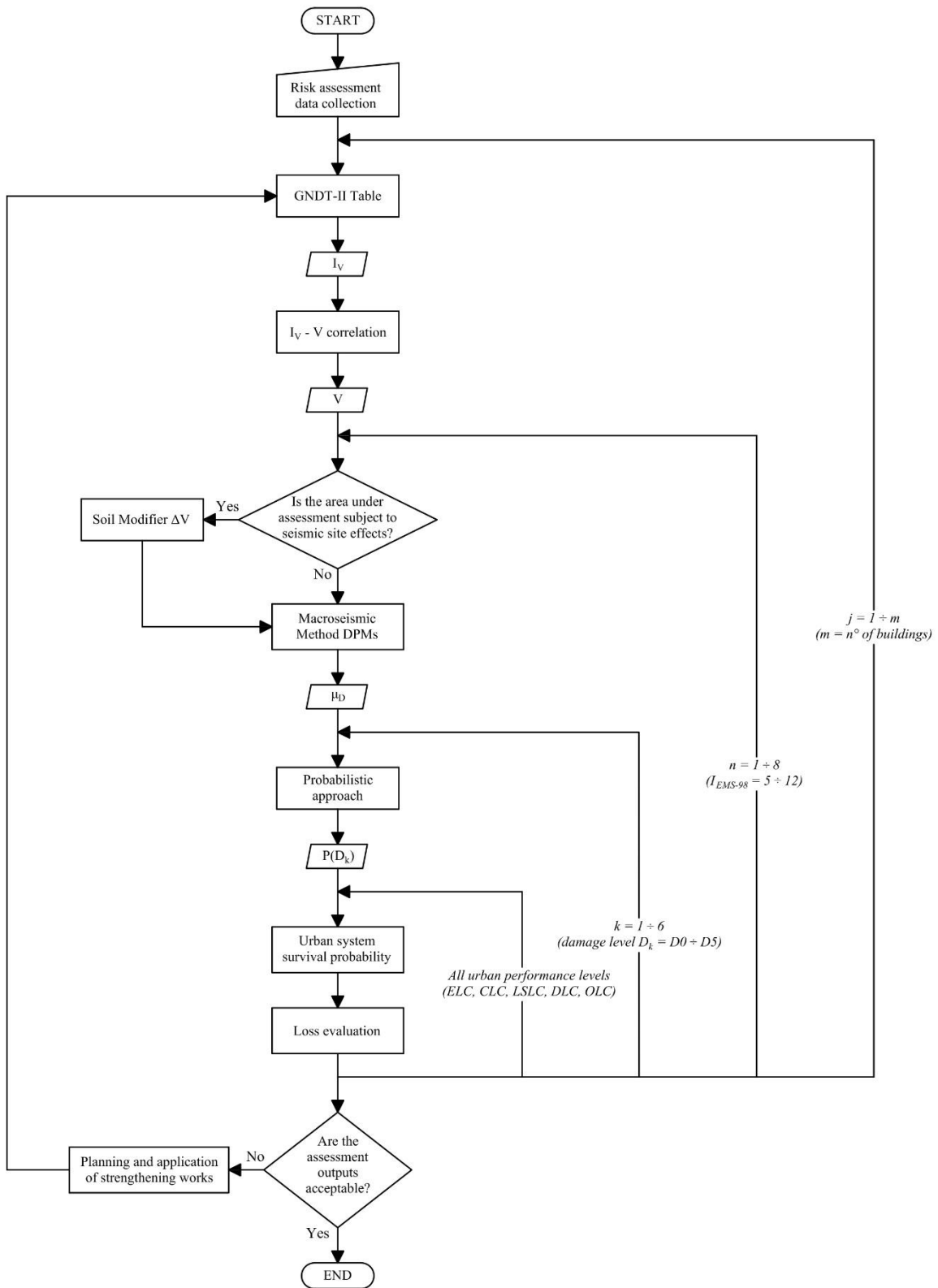
(a)

(b)

823 Fig 4. Modified Conventional Strength (Parameter 3) of the GNDT form for (a) masonry

824

buildings; (b) RC buildings.

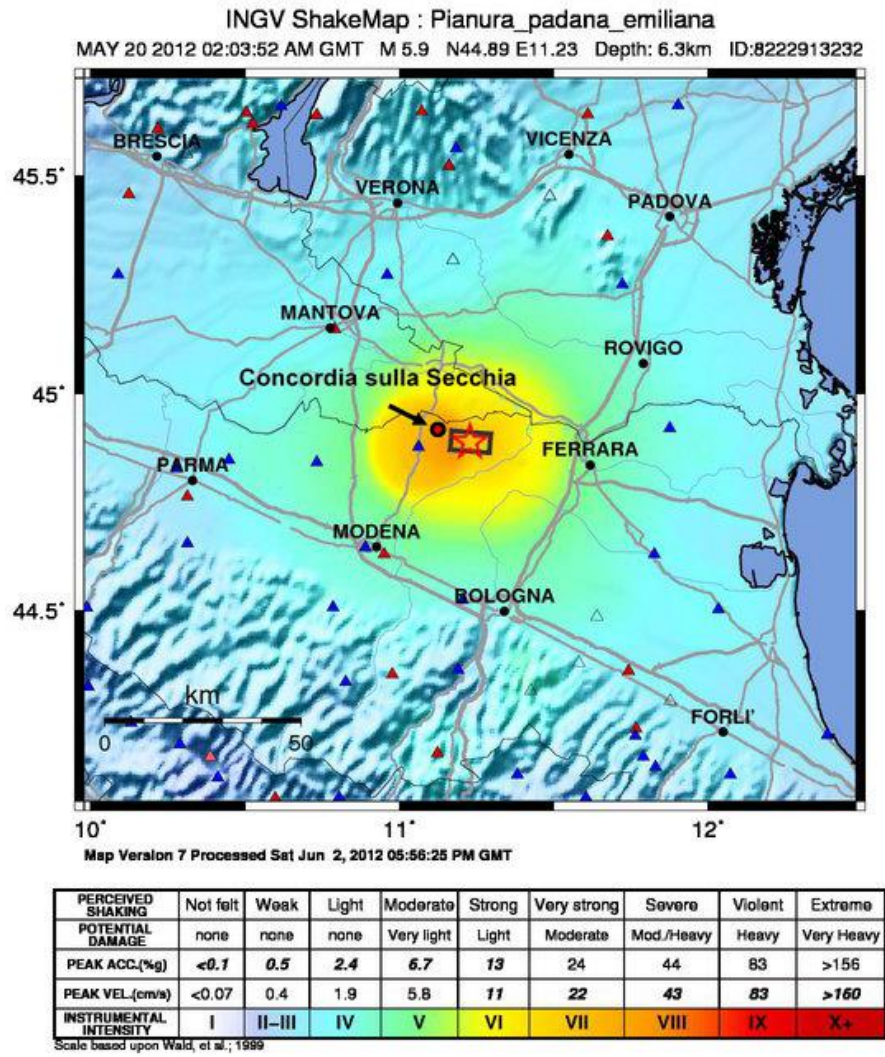


825

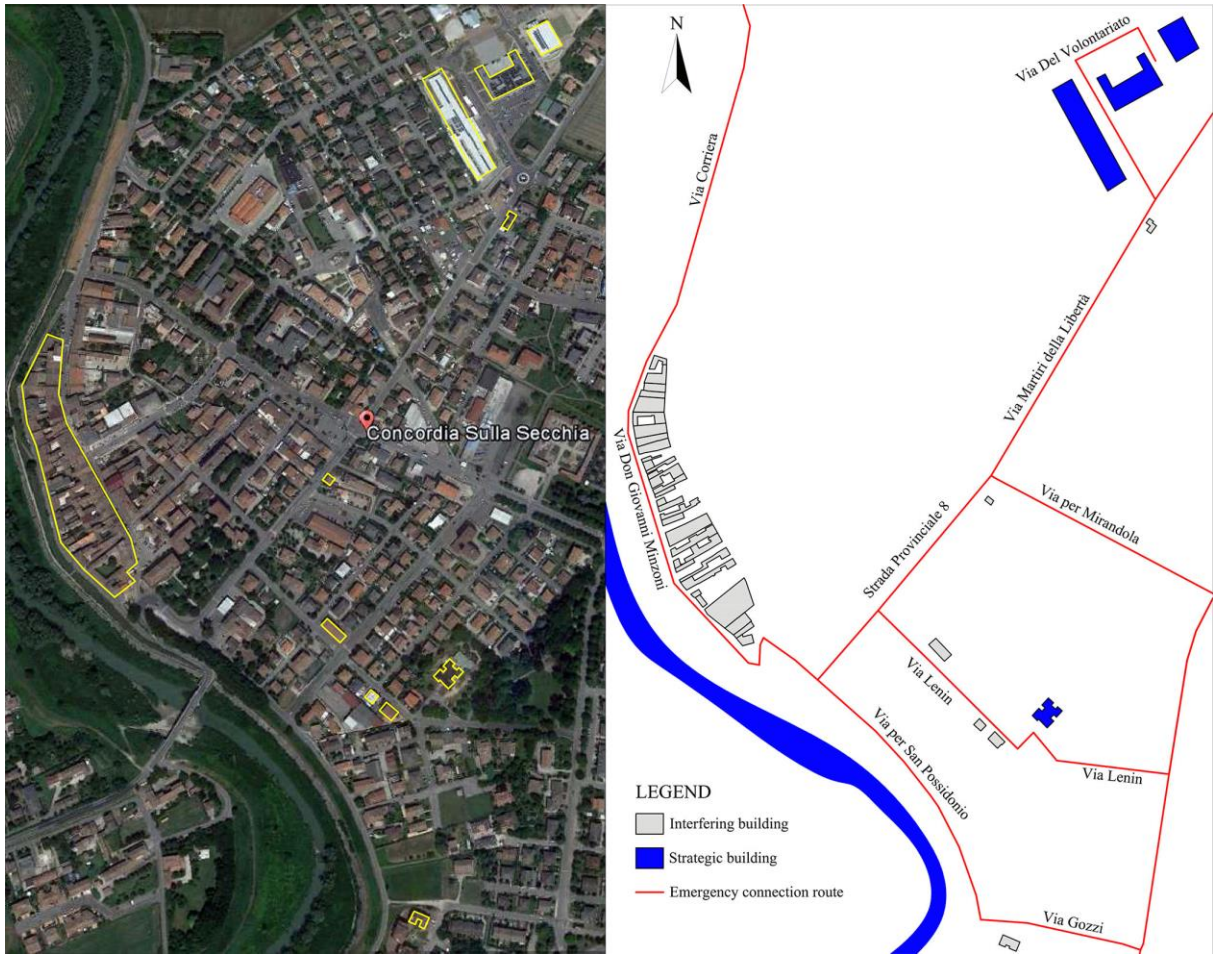
826

Fig. 5. Flowchart of the risk assessment procedure.

827



828 **Fig. 6.** Italian PPE shake map (adapted by INGV) for the Pianura Padana Earthquake of May
829 20, 2012.



830

831 **Fig. 7.** ELC plan of Concordia sulla Secchia (aerial view and location of assessed buildings).

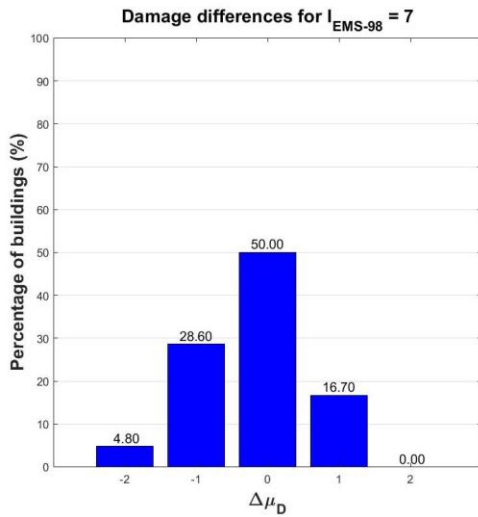
832

833

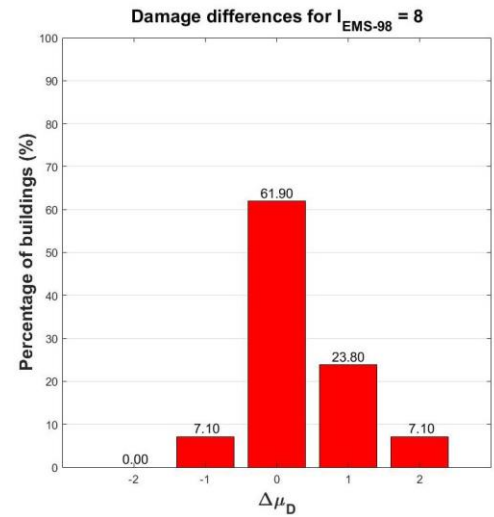
834

835

836



a)

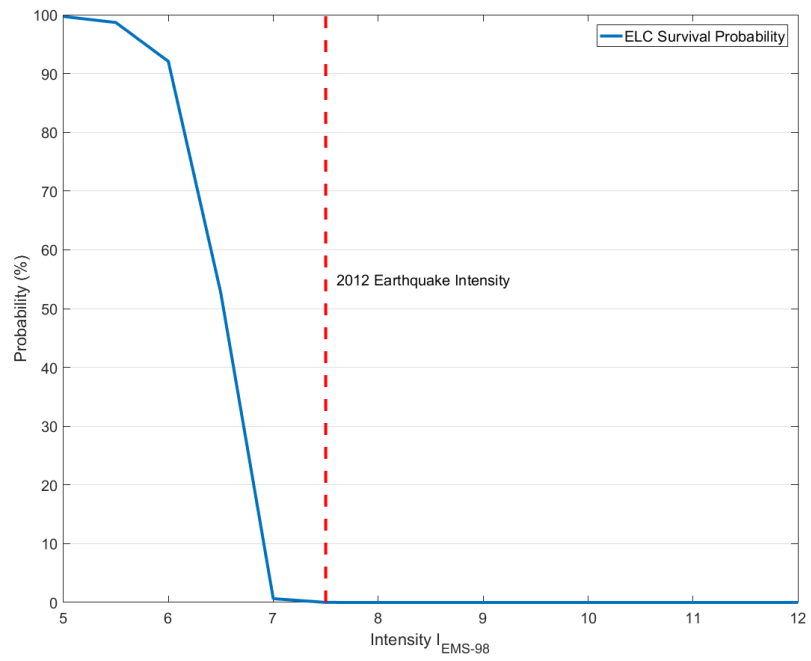


b)

Fig. 8. $\Delta\mu_D$ frequency distribution of the Concordia sulla Secchia ELC sub-system for

(a) $I_{EMS-98} = 7$; (b) for $I_{EMS-98} = 8$.

837
838
839
840
841
842
843
844
845
846
847
848
849
850
851
852
853
854
855



856 **Fig. 9.** Survival probability of the Concordia sulla Secchia ELC sub-system.

857

858

859



a)

b)

860 **Fig. 10.** Damage grade maps of the Concordia sulla Secchia ELC sub-system for **(a)**

861 $I_{EMS-98} = 7$; **(b)** for $I_{EMS-98} = 8$.

862

863

864

865

866

867

868

869

870 **LIST OF TABLES**

871 **Table I.** Vulnerability Index (I_V) for masonry buildings.

872 **Table II.** Vulnerability index (I_V) for RC buildings.

873 **Table III.** Performance levels of urban functions in different limit conditions.

874 **Table IV.** Proposed update of the vulnerability Index (I_V) additional parameters for masonry
875 buildings in aggregate sequence.

876 **Table V.** Risk assessment methodology validation. ELC sub-system of Concordia sulla
877 Secchia, hit by the 2012 Pianura Padana Earthquake.

878

879

880

881

882

883

884

885

886

887

888

889

890

891

892

893

894

895 **Table I.** Vulnerability Index (I_V) for masonry buildings.

Parameters		Class - C_{vi}				Weight w_i	Vulnerability index
		A	B	C	D		
P1	Type and organization of resisting system	0	5	20	45	1.00	$I_V^* = \sum_{i=1}^{11} C_{vi} \cdot w_i$ Normalization: $0 \leq I_V \leq 100$
P2	Quality of resisting system	0	5	25	45	0.25	
P3	Conventional strength	0	5	25	45	1.50	
P4	Building position and foundations	0	5	15	45	0.75	
P5	Horizontal diaphragms	0	5	25	45	variable *	
P6	Plan configuration	0	5	25	45	0.50	
P7	In height configuration	0	5	25	45	variable *	
P8	Maximum distance between walls	0	5	25	45	0.25	
P9	Roof	0	15	25	45	variable *	
P10	Non structural elements	0	0	25	45	0.25	
P11	General maintenance conditions	0	5	25	45	1.00	

* see GNDT-SSN, 1994 for the weight definition

896

897

898

899

900

901

902

903

904

905

906

907

908 **Table II.** Vulnerability index (I_V) for RC buildings.

Parameters	Class C_{vi}				Vulnerability index
	A	B	C	D*	
P1 Type and organization of resisting system	0	-1	-2		$I_V^* = \sum_{i=1}^{11} C_{vi}$
P2 Quality of resisting system	0	-0.25	-0.5		
P3 Conventional strength	0.25	0	-0.25		
P4 Building position and foundations	0	-0.25	-0.5		Normalization: a) if $I_V^* > -6.5$, $I_V = -10.07 \cdot I_V^* + 2.5175$ b) if $I_V^* < -6.5$, $I_V = -1.731 \cdot I_V^* + 56.72$
P5 Horizontal diaphragms	0	-0.25	-0.5		
P6 Plan configuration	0	-0.25	-0.5		
P7 In height configuration	0	-0.5	-1.5		
P8 Connections and critical elements	0	-0.25	-0.5		
P9 Low ductility elements	0	-0.25	-0.5		
P10 Non-structural elements	0	-0.25	-0.5		
P11 General maintenance conditions	0	-0.5	-1	-2.45	

* Class D is defined only for P11

909

910

911

912

913

914

915

916

917

918

919

920

921

922 **Table III.** Performance levels of urban functions in different limit conditions.

Limit state condition for urban settlement	Strategic functions for emergency *	Strategic functions for urban recovery	Main and ordinary urban functions	Residence
Operational Limit Condition (OLC)	FF	FF	FF *	FF *
Damage Limit Condition (DLC)	FF	FF	ML	ML
Life-safety Limit Condition (LSLC)	FF	FF	ML	ML
Collapse Limit Condition (CLC)	FF	ML	ML	RI
Emergency Limit Condition (ELC)	FF **	RI	RI	RI

FF: Fully Functional

ML: Marginal limitation (temporary or localized)

RI: Relevant Interruption (average-to-long term)

* accepted local losses not relevant at urban level

** most part

923

924

925

926

927

928

929

930

931

932

933

934

935 **Table IV.** Proposed update of the vulnerability Index (I_V) additional parameters for masonry
 936 buildings in aggregate sequence.

Parameters	Class C_{vi}				Weight
	A	B	C	D	p_i
P12 Presence of adjacent buildings with different height	0	15	25	45	1.25
P13 Position of the building in the aggregate	0	5	15	45	1.75
P14 Presence and number of staggered floors	0	25	35	45	0.75
P15 Effects of either structural or typological heterogeneity among adjacent structural unit	0	10	20	45	1.50
P16 Percentage difference of opening areas among adjacent facades	0	15	35	45	1.25

937

938

939

940

941

942

943

944

945

946

947

948

949

950 **Table V.** Risk assessment methodology validation. ELC sub-system of Concordia sulla
 951 Secchia, hit by the 2012 Pianura Padana Earthquake.

FID	I _v	CONSTRUCTION PERIOD (+ renovation if any)	STRUCTURAL TYPE	OBSERVED DAMAGE LEVEL INTERVAL	PREDICTED DAMAGE LEVEL		$\Delta\mu_D$	
					I = 7 (EMS-98)	I = 8 (EMS-98)	I = 7 (EMS-98)	I = 8 (EMS-98)
79	32.73	82 - 91	RC	4 - 5	2	3	-2	-1
78	61.41	72 - 81	MASONRY	4 - 5	3	4	-1	-
77	30.21	72 - 81	RC	0 - 1	2	3	+1	+2
76	37.76	72 - 81	RC	2 - 4	2	3	-	-
75	20.14	92 - 01	RC	0 - 1	1	2	-	+1
74	42.80	82 - 91	RC	1 - 2	3	3	+1	+1
73	45.32	62 - 71	RC	1 - 2	3	4	+1	+2
72	50.35	72 - 81	RC	4 - 5	3	4	-1	-
71 - 70	50.35	72 - 81	RC	4 - 5	3	4	-1	-
69	22.66	92 - 01	RC	1 - 2	1	2	-	-
68	22.66	62 - 71	RC	2 - 4	1	2	-1	-
67 - 1	35.25	92 - 01	RC	1 - 2	2	3	-	+1
67 - 2	22.66	92 - 01	RC	1 - 2	1	2	-	-
66 - 1	52.87	< 1919 + 92 - 01	RC	4 - 5	3	4	-1	-
66 - 2	32.73	< 1919 + 92 - 01	RC	4 - 5	2	3	-2	-1
63	66.08	72 - 81	MASONRY	4 - 5	3	4	-1	-
64	57.14	92 - 01	MASONRY	4 - 5	3	4	-1	-
65	50.35	< 1919	RC	1 - 2	3	4	+1	+2
61	60.42	19 - 45	RC	4 - 5	4	4	-	-
60	25.18	72 - 81	RC	0 - 1	1	2	-	+1
59	50.35	72 - 81	RC	2 - 4	3	4	-	-
106	35.28	72 - 81	MASONRY	1 - 2	2	3	-	+1
105	61.82	72 - 81	MASONRY	4 - 5	3	4	-1	-
104	55.17	19 - 45	MASONRY	4 - 5	3	4	-1	-
58	47.07	< 1919	MASONRY	2 - 4	2	3	-	-
57	50.71	< 1919	MASONRY	2 - 4	3	4	-	-
56	25.18	92 - 01	RC	2 - 4	2	2	-	-
55	32.73	82 - 91	RC	2 - 4	2	3	-	-
54	40.28	92 - 01	RC	4 - 5	3	3	-1	-1
53 - 52	45.32	62 - 71	RC	2 - 4	3	4	-	-
51	37.76	62 - 71	RC	2 - 4	2	3	-	-
29	45.32	46 - 61 + 72 - 81	RC	4 - 5	3	4	-1	-
33	25.99	62 - 71	RC	0 - 1	2	2	+1	+1
32	27.23	19 - 45	RC	0 - 1	2	2	+1	+1
31	35.48	> 2002	RC	2 - 4	2	3	-	-
30	38.12	46 - 61 + 72 - 81	RC	1 - 2	2	3	-	+1
34	46.59	62 - 71	RC	4 - 5	3	4	-1	-
35	24.14	92 - 01 + > 2002	RC	0 - 1	1	2	-	+1
113	25.38	72 - 81	RC	0 - 1	2	2	+1	+1
111	0.1	> 2002 (2012)	STEEL	0 - 1	0	1	-	-
110	0.1	> 2002 (2012)	MIXED	0 - 1	0	1	-	-
112	0.1	> 2002 (2013)	STEEL	0 - 1	0	1	-	-

952